Crystal-field model of the $Pb^0(2)$ centre in SrF_2

1989 J. Phys.: Condens. Matter 1 27

(http://iopscience.iop.org/0953-8984/1/1/003)

J. Phys.: Condens. Matter **1** (1989) 27–34. Printed in the UK

Crystal-field model of the $Pb^0(2)$ centre in SrF_2

R H Bartram†, M Fockele‡, F Lohse‡ and J-M Spaeth‡

† Department of Physics and Institute of Materials Science, University of Connecticut, Storrs, CT 06268, USA

‡ Fachbereich Physik, Universität-GH Paderborn, Warburger Strasse 100A, D-4790 Paderborn, Federal Republic of Germany

Received 20 June 1988

Abstract. A crystal-field model of the $Pb^0(2)$ centre in SrF_2 accounts for a metastable state which is the source of luminescence, as well as for three peaks observed in its excitation spectrum. Both transition energies and relative intensities are predicted correctly within experimental error. Adjusted values of the spin–orbit constant and a Slater integral are reduced by 21% from their free-atom values. The adjusted values of the axial crystal-field parameter γ in the relaxed ground state and metastable excited state are 0.6529 eV and 0.5213 eV, respectively. A Huang–Rhys factor $S_0 = 12$ and a phonon energy $\hbar\omega = 90\ cm^{-1}$ are inferred from the calculated energy of the metastable state and from the position and width of the observed emission band.

1. Introduction

The $Pb^+(1)$ centre in alkaline-earth halides, consisting of a substitutional Pb^+ ion adjacent to a halogen vacancy, is the analogue of the laser-active $Tl^0(1)$ centre in alkali halides. Efficient fluorescence has been predicted for this centre (Fockele *et al* 1989) on the basis of the Dexter–Klick–Russell rule, as elaborated by Bartram and Stoneham (1975) and has been found in the alkaline-earth fluorides (Fockele *et al* 1989).

The initial failure of $Pb^+(1)$ centres in SrF_2 to exhibit laser gain (Huber 1987) has been attributed to the presence of an additional colour centre which absorbs at the emission wavelength of the $Pb^+(1)$ centre. Three excitation bands and an infrared emission band have been identified for this additional centre. From its observed properties (a low oscillator strength, a long luminescence lifetime of 10 ms at 10 K in SrF_2 and the absence of a paramagnetic resonance signal (Fockele *et al* 1989)), it has been tentatively identified as a $Pb^0(2)$ centre, consisting of a neutral Pb atom at a cation site flanked by a pair of anion vacancies along a ⟨111⟩ direction, as illustrated in figure 1. With the structure as shown, in which the Pb atom occupies a site of inversion symmetry, all electric dipole transitions within the ground-state electronic configuration of the $Pb^0(2)$ centre would be forbidden by the Laporte selection rule. In order to account for the weak absorption actually observed, we postulate an off-centre displacement of the Pb atom along the line joining the two anion vacancies in the ground-state equilibrium configuration.

0953-8984/89/010027 + 08 $02.50

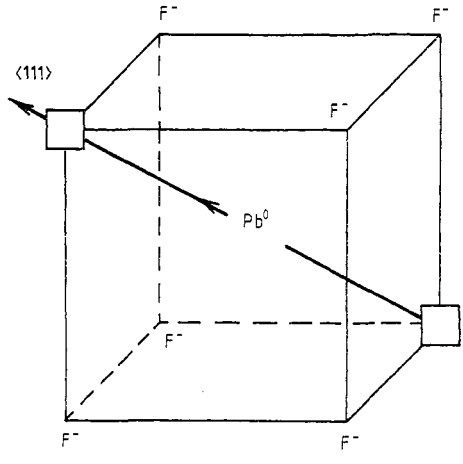

Figure 1. Geometrical configuration of the $Pb^0(2)$ centre in SrF_2, consisting of a substitutional Pb atom with two adjacent anion vacancies along a ⟨111⟩ direction.

We have undertaken to calculate the properties of the $Pb^0(2)$ centre on the basis of a phenomenological description incorporating several adjustable parameters. The purpose of this undertaking is to verify that the model can in fact explain the data, and to identify the transitions involved in the measured spectra.

2. Crystal-field model

The $Pb^0(2)$ centre in its assumed configuration has C_{3v} symmetry. The computational model adopted in this work incorporates a simplified crystal field of symmetry $C_{\infty v}$ with a single adjustable parameter γ, as in analogous treatments of $Tl^0(1)$ centres (Mollenauer *et al* 1983). However, the case of the $Pb^0(2)$ centre is complicated by the presence of two 6p electrons in the ground-state configuration. We adopt a non-relativistic Hamiltonian H for these two electrons which includes spin–orbit interaction as well as their interaction with the central potential $U(r)$ of the Pb^{2+} core, with the external crystal field and with one another:

$$H = \sum_{i=1,2} \left(\frac{-\hbar^2}{2m} \nabla_i^2 + U(r_i) + \zeta \boldsymbol{l}_i \cdot \boldsymbol{s}_i + \gamma[3l_{iz}^2 - l(l+1)] \right) + \frac{e^2}{r_{12}}. \qquad (1)$$

For transition-metal ions in solids, the spin–orbit interaction is much weaker than the crystal field and can be treated by first-order perturbation theory within a single crystal-field term (Sugano *et al* 1970). That inequality is reversed for rare-earth ions in solids, where the crystal field can be treated by first-order perturbation theory within each fine-structure level (Hüfner 1978). Because of the position of Pb in the periodic table and the extended nature of its 6p orbitals, the electrostatic interaction of its two electrons is comparable with both their spin–orbit interaction and their interaction with the external crystal field. Consequently, the simplifying approximations employed for transition-metal and rare-earth ions in solids are inapplicable in the present case, and it is essential to diagonalise matrices of all three interactions simultaneously within the entire ground-state configuration.

The effect of each of these interactions on the energy level structure of the ground-state configuration is illustrated in figure 2 by introducing them in sequence. The mutual

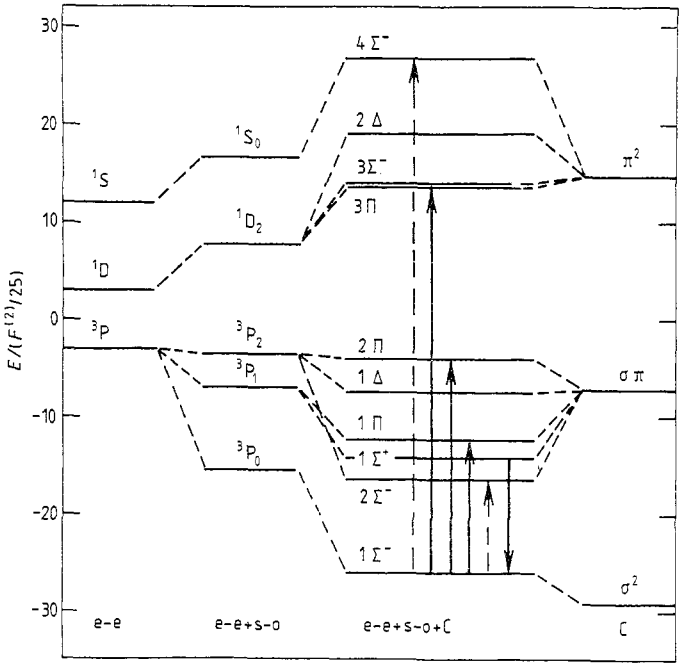

Figure 2. Energy level scheme for the $Pb^0(2)$ centre in SrF_2, illustrating the sequential effects within the ground-state configuration of electron–electron (e–e) interaction, spin–orbit (s–o) interaction and interaction with an axial crystal field (C). The solid vertical lines denote transitions identified with peaks in the excitation spectrum and with the luminescence band.

electrostatic interaction of the two 6p electrons splits the ground-state configuration into three terms: ^3P, ^1D and ^1S in order of increasing energy. Spin–orbit interaction further splits the ground term into fine-structure levels: $^3P_0$, $^3P_1$ and $^3P_2$, in ascending order. However, since the $^3P_0$ and $^3P_2$ states interact strongly with the $^1S_0$ and $^1D_2$ states, respectively, only J and M_J remain as valid quantum numbers. Finally, the fine-structure levels are split by the axial crystal field. The quantum number M_J remains valid, and irreducible representations of $C_{\infty v}$ which label the energy levels are distinguished by means of $\Omega = |M_J|^2$. For the special case $\Omega = 0$, they are further distinguished as Σ^+ and Σ^- according to whether the wavefunction is even or odd on reflection in a plane containing the symmetry axis (Weissbluth 1978). States of each symmetry are numbered in ascending order of energy in figure 2. Note that there is only one Σ^+ state in the ground-state configuration, derived from the $M_J = 0$ component of the $^3P_1$ fine-structure level. The corresponding A_1 representation in C_{3v} symmetry labels just one state as well; the remaining correspondences are $\Sigma^- \leftrightarrow A_2$, and $\Pi, \Delta \leftrightarrow E$.

Electric dipole transitions are allowed from the Σ^- ground state to the excited Σ^- and Π states, with polarisation parallel and perpendicular, respectively, to the symmetry axis. The three peaks observed in the measured excitation spectrum are ascribed to the transitions from the $1\Sigma^-$ ground state to the 1Π, 2Π, 3Π and $3\Sigma^-$ excited states, with the third and fourth transitions unresolved. (The energy-level separation in figure 2 is drawn to scale, anticipating numerical results presented in subsequent sections.) The transition $\Sigma^+ \rightarrow \Sigma^-$ is rigorously forbidden, as is the corresponding $A_1 \rightarrow A_2$ transition in C_{3v} symmetry; accordingly, the $1\Sigma^+$ state is identified as the metastable emitting state. This

state is stable against non-radiative de-excitation to the lower $1\Sigma^-$ and $2\Sigma^-$ states, as well, since a Σ^- promoting mode required to mediate such non-radiative transitions cannot exist; a set of atomic displacements which is invariant under rotation about the symmetry axis must necessarily be invariant under reflection in a plane containing that axis. The analogous A_2 promoting mode in C_{3v} symmetry is similarly prohibited. The lowest allowed transition, $1\Sigma^- \rightarrow 2\Sigma^-$, does not appear in the excitation spectrum since its final state lies below the emitting state, and the transition $1\Sigma^- \rightarrow 4\Sigma^-$ is presumed to be weak.

3. Energy levels

The measured energy level structure of the free Pb atom can be described approximately within the ground-state configuration in terms of two parameters: a spin–orbit constant ζ and a Slater integral $F^{(2)}$ (Slater 1960). Since both ζ and $F^{(2)}$ are expected to be somewhat decreased by incorporation of the Pb atom in a solid host crystal, these two parameters are readjusted for the $Pb^0(2)$ centre. The crystal-field parameter γ is also adjusted. The energy matrices, absent terms common to the entire ground-state configuration, are listed in table 1 in units of $F^{(2)}/25$, in an $|LSJM_J\rangle$ representation. They are expressed in terms of reduced variables $x = \zeta/(F^{(2)}/25)$ and $y = \gamma/(F^{(2)}/25)$.

Energy levels associated with the ground-state configuration of the free Pb atom are obtained by diagonalising the matrices in table 1 with $\gamma = 0$. The free-atom energies

Table 1. Energy matrices in an $|LSJM_J\rangle$ representation, in units of $F^{(2)}/25$. Parameters are defined as $x = \zeta/(F^{(2)}/25)$ and $y = \gamma/(F^{(2)}/25)$.

$M_J = 2$

	$^1D_2$	$^3P_2$
$^1D_2$	$3 + 2y$	$x/2^{1/2}$
$^3P_2$	$x/2^{1/2}$	$-3 + x/2 - y/2$

$M_J = 1$

	$^1D_2$	$^3P_2$	$^3P_1$
$^1D_2$	$3 - y$	$x/2^{1/2}$	0
$^3P_2$	$x/2^{1/2}$	$-3 + x/2 + y/2$	$-3y/2$
$^3P_1$	0	$-3y/2$	$-3 - x/2 + y/2$

$M_J = 0$

	$^1D_2$	$^3P_2$	$^3P_0$	$^1S_0$	$^3P_1$
$^1D_2$	$3 - 2y$	$x/2^{1/2}$	0	$2^{3/2}y$	0
$^3P_2$	$x/2^{1/2}$	$-3 + x/2 + y$	$2^{1/2}y$	0	0
$^3P_0$	0	$2^{1/2}y$	$-3 - x$	$-2^{1/2}x$	0
$^1S_0$	$2^{3/2}y$	0	$-2^{1/2}x$	12	0
$^3P_1$	0	0	0	0	$-3 - x/2 - y$

Table 2. Comparison of calculated differences of free-atom energy eigenvalues with experimental values (Moore 1958). The optimised parameters for this calculation are listed in table 3.

Energy difference	Theory (cm^{-1})	Experiment (cm^{-1})
$E(^1S_0) - E(^3P_0)$	29490	29466.81
$E(^1D_0) - E(^3P_0)$	21320	21457.90
$E(^3P_2) - E(^3P_0)$	10840	10650.47
$E(^3P_1) - E(^3P_0)$	7860	7819.35

listed in table 2 were calculated with ζ and $F^{(2)}$ adjusted for a least-squares fit to experimental values (Moore 1958), which are also listed for comparison. It can be seen that an excellent fit is obtained; neglect of configuration mixing and relativistic corrections is evidently compensated for by the parameter adjustment. The optimum values of the parameters are listed in table 3.

Energy levels derived from the ground-state configuration of the Pb atom are plotted in figure 3 as functions of the reduced crystal-field parameter y with x fixed at its optimum value for the free atom, $x = 7.941$. The optimum value of y, obtained by a least-squares fit, with fixed x, of the ratios of predicted transition energies to the values determined from excitation spectra, is $y = 7.322$. The corresponding optimum values of the parameters ζ, γ and $F^{(2)}$ are listed in table 3, and the calculated transition energies are compared with experiment in table 4. The transition energy corresponding to the shortest-wavelength excitation band was taken to be the average of those for the $1\Sigma^- \rightarrow 3\Pi$ and $1\Sigma^- \rightarrow 3\Sigma^-$ transitions, weighted by the calculated transition probabilities presented in § 4. As noted previously, the $1\Sigma^- \rightarrow 2\Sigma^-$ transition is not expected to appear in the excitation spectrum since the $2\Sigma^-$ state lies below the $1\Sigma^+$ emitting state. The failure to observe it in the absorption spectrum (Fockele *et al* 1988) can also be regarded as within experimental error, since it is very difficult to observe a weak transition in that wavelength region.

The crystal-field levels can be classified alternatively by the strong-field configurations $\lambda_1\lambda_2$ and fine-structure levels $^{2S+1}\Lambda_\Omega$ to which they tend in the limit in which the crystal field is the dominant interaction; these labels are also shown in figure 3. It should be noted that the singlet spin function is odd on reflection in a plane containing the symmetry axis; consequently, a $^1\Sigma^+$ state in the strong-field limit has overall symmetry

Table 3. Values of adjusted parameters.

		$Pb^0(2)$ centre	
Parameter (units)	Free atom	Absorption	Emission
x	7.941	7.941	7.941
y	0	7.322	5.847
$F^{(2)}/25$ (cm^{-1})	918.4	721.5	721.5
ζ (cm^{-1})	7293	5730	5730
γ (cm^{-1})	0	5282	4218
γ (eV)	0	0.6529	0.5213

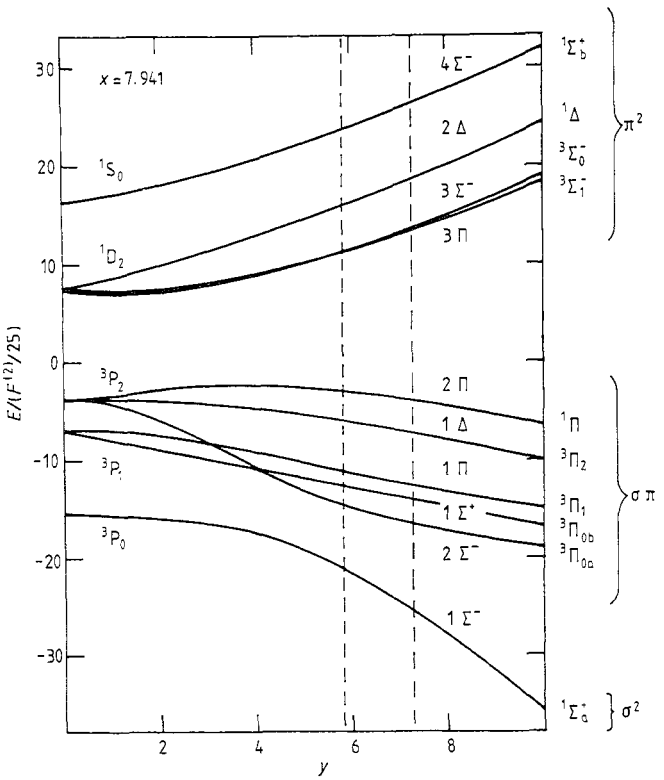

Figure 3. Calculated energy levels derived from the ground-state configuration of the Pb atom, plotted in units of the Slater integral, $F^{(2)}/25$, as a function of the reduced crystal-field parameter $y = \gamma/(F^{(2)}/25)$. The reduced spin–orbit parameter $x = \zeta/(F^{(2)}/25)$ is fixed at its optimum value for the free atom, $x = 7.941$. The vertical broken lines indicate the optimum values of y in emission and absorption. The energy levels are labelled by the irreducible representations of $C_{\infty v}$; additional labels designate free-atom fine-structure levels on the left and strong-field terms and configurations on the right.

Σ^-. Since only the $1\Sigma^- \rightarrow 2\Pi$ transition corresponds to an allowed transition in the strong-field limit, it is expected to be associated with the most prominent excitation band.

Table 4. Comparison of calculated transition energies and relative transition probabilities with positions and relative intensities, respectively, of peaks in the excitation spectrum (Fockele *et al* 1988). The optimised parameters for this calculation are listed in table 3.

Transition (absorption)	Transition energy (cm^{-1})		Relative intensity	
	Theory	Experiment	Theory	Experiment
$1\Sigma^- \rightarrow 4\Sigma^-$	37990	—	0.028	—
$1\Sigma^- \rightarrow 3\Pi, 3\Sigma^-$	28700	28700	0.329	0.41
$1\Sigma^- \rightarrow 2\Pi$	15850	15850	0.640	0.64
$1\Sigma^- \rightarrow 1\Pi$	9830	9825	0.366	0.32
$1\Sigma^- \rightarrow 1\Sigma^+$	8500	—	0.000	—
$1\Sigma^- \rightarrow 2\Sigma^-$	6790	—	0.137	—

4. Transition probabilities

In order to complete the comparison of our crystal-field model with experiment, we have endeavoured to predict relative integrated intensities of the excitation bands. For this purpose, it is assumed that the transition probabilities for the excitation of luminescence are identical with those for absorption. However, it should be remarked that the excited Σ^- states can relax non-radiatively to the $1\Sigma^+$ state only by an indirect process via Π states; consequently, optical transitions to Σ^- states may be less effective in exciting luminescence than those directly to Π states.

The postulated off-centre displacement of the Pb atom in the ground state relaxes the Laporte selection rule by mixing 6s and 6p orbitals. This weak orbital admixture is obscured in the energy level calculation by neglect of configuration mixing but is essential to the determination of transition probabilities. Only 6s and $6p_z$ orbitals are mixed when the z direction is chosen parallel to the crystal-field axis. Probabilities for all allowed transitions are proportional to the square of the product of the admixture coefficient and the matrix element of the dipole moment operator between 6s and 6p orbitals. No attempt has been made to evaluate this factor; we have concentrated on relative transition probabilities instead. We proceeded by evaluating matrix elements of the dipole moment operator in an $|LSJM_J\rangle$ representation and then transforming to the intermediate-coupling representation specified by the eigenvectors of the matrices listed in table 1, evaluated for the optimum values of the parameters x and y. The calculated relative transition probabilities are listed, in arbitrary units, in table 4, where they are compared with relative intensities of peaks in the excitation spectrum.

5. Discussion

A crystal-field model of the postulated $Pb^0(2)$ centre is found to provide transitions corresponding both to observed peaks in the excitation spectrum and to the phosphorescent emission band. It is evident from table 4 that adjustment of the parameters $F^{(2)}$ and $y = \gamma/(F^{(2)}/25)$ with a fixed value of $x = \zeta/(F^{(2)}/25)$ yields values of transition energies in virtually precise agreement with observed excitation bands. The adjusted values of ζ and $F^{(2)}$ listed in table 3 show a modest (21%) reduction from free-atom values, consistent with expectations.

The calculated relative transition probabilities listed in table 4 agree with the relative intensities of peaks in the excitation spectrum within experimental error. Furthermore, the unobserved $1\Sigma^- \rightarrow 4\Sigma^-$ transition is predicted to have a very low relative transition probability, as conjectured. Although there is no *a priori* reason to assume a fixed value of x, the quality of agreement with both transition energies and intensities is such that no further parameter variation is justified.

The lowest-energy excitation band exhibits resolved vibronic structure corresponding to weak coupling to a vibrational mode of phonon energy $\hbar\omega_{ex} = 6$ meV (50 cm^{-1}) (Fockele *et al* 1989). With the assumption of linear coupling, a value for the zero-temperature Huang–Rhys factor S_0 can be inferred from the ratio of the integrated intensity of the zero-phonon line to that of the entire band, $\exp(-S_0)$ (Stoneham 1975). For the lowest excitation band, $S_{0ex} = 3$. The low vibration frequency suggests a mode in which displacement of the Pb atom predominates. The origin of coupling to such a mode can be understood with reference to figure 3. Off-centre displacement of the Pb

atom intensifies the crystal field and reduces the ground-state energy. Since the energy of the 1Π excited state is much less sensitive to the crystal field than that of the $1\Sigma^-$ ground state, a much smaller equilibrium displacement is expected in the excited state.

The observed properties of the emission band are also compatible with the model. The long luminescence lifetime is explained by the fact that the transition is strictly dipole forbidden in both cylindrical and trigonal symmetry and is stable against non-radiative de-excitation as well. The observed emission energy of 6250 cm^{-1} is consistent with a value $y = 5.847$ in the relaxed excited state; the corresponding value of γ is listed in table 3. Since the final state in absorption differs from the initial state in emission, it is permissible to assume linear coupling for both transitions, but to different modes. (The data are insufficient to support an interpretation in terms of non-linear coupling.) In the absence of resolved vibronic structure, the parameters S_0 and $\hbar\omega$ for the emission band must be determined more indirectly. With the assumption of linear coupling, the difference between the calculated energy separation of the $1\Sigma^+$ and $1\Sigma^-$ states and the observed transition energy is the predicted Stokes shift $\Delta E = 2250\ cm^{-1}$, given by

$$\Delta E = 2S_0\hbar\omega. \tag{2}$$

(The Stokes shift in this case is with respect to a hypothetical $1\Sigma^- \rightarrow 1\Sigma^+$ transition which is in fact forbidden.) An additional low-temperature relation involving these quantities is obtained from the full width of the emission band at half-maximum (FWHM) which equals 750 cm^{-1} at 10 K (Fockele *et al* 1988):

$$\text{FWHM}^2 = 8 \ln 2\, S_0(\hbar\omega)^2. \tag{3}$$

It follows from equations (2) and (3) that, for the emission band, $S_{0em} = 12$ and $\hbar\omega_{em} = 90\ cm^{-1}$. These values suggest relatively strong coupling to modes involving displacement of host lattice ions and are consistent with the absence of resolved vibronic structure.

We conclude that the $Pb^0(2)$ centre provides a consistent qualitative and quantitative explanation of the observed spectra and thus fully supports the identification of this centre.

Acknowledgments

This work was supported in part by the US Army Research Office under Contract DAAL03-86-K-0017, and in part by the North Atlantic Treaty Organisation under Grant RG.85/0662.

References

Bartram R H and Stoneham A M 1975 *Solid State Commun.* **17** 1593

Fockele M, Lohse F, Spaeth J-M and Bartram R H 1989 *J. Phys.: Condens. Matter* **1** 13

Huber G 1987 private communication

Hüfner S 1978 *Optical Spectra of Transparent Rare Earth Compounds* (New York: Academic)

Mollenauer L F, Vieira N D and Szeto L 1983 *Phys. Rev.* B **27** 5332

Moore C E 1958 *Atomic Energy Levels* vol III, NBS Circular No 467 (Washington, DC: US Government Printing Office) p 208

Slater J C 1960 *Quantum Theory of Atomic Structure* vol II (New York: McGraw-Hill)

Stoneham A M 1975 *Theory of Defects in Solids* (Oxford: Clarendon)

Sugano S, Tanabe Y and Kamimura H 1970 *Multiplets of Transition-Metal Ions in Crystals* (New York: Academic)

Weissbluth M 1978 *Atoms and Molecules* (New York: Academic)